



---

## **Electrochemical Fabrication of Randomly Nanoarrayed Electrodes to Enhance Sensitivity and Selectivity of Sensors**

Abiyot Kelecha Geletu<sup>a\*</sup>, Tesfaye Refera Soreta<sup>b</sup>

<sup>a</sup>*Department of Chemistry, Faculty of Natural and Computational Sciences, Mettu University, Mettu, Ethiopia*

<sup>b</sup>*Department of Chemistry, College of Natural Science, Jimma University, Jimma, Ethiopia*

<sup>a</sup>*Email: abitk2005@gmail.com*

<sup>b</sup>*Email: tesfaye.referat@ju.edu.et or tesfishr2001@yahoo.com*

### **Abstract**

Increasing sensitivity and selectivity, as well as, long-term durability of electrochemical sensors are the reasons for designing active layers on electrodes. Significant advances in this field originate from the chemical approach to nanotechnology, involving bottom-up synthetic pathways to generate nanostructured materials on electrode surfaces. In this work randomly nanoarrayed electrodes were fabricated and electrochemically characterized. This was achieved by depositing gold nanoparticles, AuNPs on bare glassy carbon, from 0.1 mmol/L KAuCl<sub>4</sub> in H<sub>2</sub>SO<sub>4</sub> using chronoamperometry followed by surface passivation through reduction of in situ prepared nitrophenyl diazonium cation. To increase the number of nucleated metal nanoparticles self assembly monolayers (SAMs) of 2-mercaptoethanol (2-ME) was used during three deposition steps. The nitrophenyl grafted film was characterized by cyclic voltammetry and has shown a significant blocking property towards Fe(CN)<sub>6</sub><sup>3-</sup> probe. The nanoholes were produced by stripping the deposited gold nanoparticles (AuNPs) and their response to common probes such as hydroquinone and ruthenium hexamine chloride were studied at different scan rates in comparison with the signal obtained at bare glassy carbon. The improvement in selectivity is attributed to controlling the charge of insulation layer made from nitrophenyl film.

---

\* Corresponding author.

Determination of dopamine hydrochloride, DA and Chlorpromazine hydrochloride, CPZ was made with their respective limit of detection  $7.4 \times 10^{-8}$  mol/L and 8.5 mol/L measured over concentration ranges of  $9.9 \times 10^{-7}$  mol/L –  $3.4 \times 10^{-5}$  mol/L and  $7.96 \times 10^{-6}$  mol/L –  $2 \times 10^{-4}$  mol/L, respectively. The limits of detection for DA, CPZ and ascorbic acid, AA, on unmodified (bare) GC electrode were  $1.02 \times 10^{-7}$  mol/L,  $1.05 \times 10^{-7}$  mol/L, and  $1.1 \times 10^{-7}$  mol/L, respectively. The developed method can be applied in selective determination of cationic drugs where anionic species interfere.

**Keywords:** dopamine; grafting; electro deposition; randomly arrayed nanoelectrodes.

## 1. Introduction

Modifying the surface of electrodes to provide some control over how the electrode interacts with its environment has been one of the most active areas of research interest in electrochemistry during the last decade [1]. With recent developments in fabrication technologies, the size of ultramicroelectrodes (UMEs) can be reduced down to the nanometer scale [2]. Advances in surface nanostructuring started with well-ordered self-assembled monolayers [3] but many other examples are now available and described in well-documented reviews, including nanostructured films prepared by layer-by-layer self-assembly[4], metal nanotube membranes or nanoelectrode ensembles [5], or devices based on surface confinement of nanoparticles, nanowires or nanotubes [6] (especially gold nanoparticles) and carbon nanotubes [7].

The primary reason for use of ultramicroelectrodes and smaller electrodes is the benefit obtained from the enhanced mass transport of analyte towards the electrode. As electrodes decrease in size, radial (3-dimensional) diffusion becomes dominant and results in faster mass transport. Nanoelectrode arrays are of particular interests for analytical applications due to their ease of use and high reliability. Detection sensitivity for small electroactive species down to the nM regime has been demonstrated using nanoelectrode arrays fabricated in nanotemplates [6]. The size and the spatial distribution were found to be critical for the performance of the array [8-11]. However, these parameters are not independently controlled with current fabrication approaches [12, 13]. Progress in nanoelectrode research is, as one might expect, directly correlated to progress in fabrication and characterization of these nanostructures. Electrode geometry and that of the insulating protective cover surrounding the electrode are issues as important as actual electrode size, since they determine the mass transport of electroanalytes [14, 15] and thereby the proper interpretation of currents and current-potential curves.

Nanoelectrode ensembles (NEEs) have been the subject of investigation by Martin and co-workers [16]. They have prepared disc arrays by the electrodeposition of metals within the micrometre and sub-micrometre-sized pores of polymeric porous membranes using the template synthesis method. A further approach to nanoelectrode ensembles/nanoelectrode arrays is to insulate a planar electrode and then open up holes in that insulation layer through to the underlying electrode.

Nanoelectrode arrays have been fabricated by creating high-aspect-ratio pores through an alumina insulating layer using an I<sub>2</sub> gas-assisted focused-ion-beam (FIB) milling, ion beam sculpting, and electrodeposition of Au

[17]. It was observed that cyclic voltammetry calibration with a standard redox species exhibits a significant increase of current density by two orders of magnitude compared to that obtained from a microelectrode. In the works of Doescher and his colleagues [18] gold nanowell electrode arrays, with a depth of approximately 50 nm, have been prepared. The electrodes were prepared by the electrodeposition of gold through the pores of a porous alumina membrane. Both electrochemical gold stripping and ion bombardment were employed to remove gold to create the wells, with the best results obtained from a combination of these techniques. Xiao and coworkers [19] have constructed a random array of boron doped diamond (BDD) nano-disc electrodes (RAN BDD), formed by electrodeposition of molybdenum(IV) dioxide nanoparticles on to BDD substrate. The electrode surface was covered in an insulating polymer film by the electropolymerization of a 4-nitrophenyldiazonium salt. The molybdenum dioxide nanoparticles are then dissolved from the BDD surface (removing the polymer layer directly above them only) using dilute hydrochloric acid to expose nano-discs of BDD, *ca.* 20±10 nm in diameter surrounded by a polymer insulating the remainder of the BDD. Moreover, it was found that at modest scan rates the RAN BDD array was found to produce peak currents approaching that of the Randles–Sevcik limit for the equivalent geometric electrode area with significantly reduced capacitive background current compared to the bare BDD electrode.

Electrodeposition is an alternative way to produce nanostructures on an electrode surface from solution onto a surface. Using electrodeposition to construct nanostructures allows for greater control over the amount of material deposited on the surface due to the ability to precisely control the charge that is passed into the system. Liu and his colleagues [20] demonstrated the production of pyramidal, rod-like and spherical gold structures on gold foil. The production of these nanostructures was simply achieved by electrodeposition of gold from an aqueous solution of 0.1 M HClO<sub>4</sub> and different concentrations of HAuCl<sub>4</sub>.

The interactions between molecules and surfaces are some of the most exciting and widely studied aspects of modern surface science [21, 22]. Surface modification of conducting or semiconducting substrates can be used for the production of new superior products in terms of increased corrosion resistance, better biocompatibility, and improvement of optical and electrical/electronic properties. Organic thin films are of prime technological interest, as the presence of molecules chemically bound to the surface renders the properties of the modified interface (i.e., wetting, conductivity, adhesion, and chemistry) to be entirely different from those of the bare substrate. Some of the commonly used methods for surface passivation include grafting of dizonium salts, protection by self-assembled monolayers (SAMs), the most popular being citrate and thiol-functionalized organics; encapsulation in the water pools of reverse microemulsions [21].

However, few works have been reported so far on nanoelectrode ensemble fabrication based on electronucleation of metal nanoparticles and hence the present work aims at electrochemical fabrication with the same approach as Xiao and coworkers [19] but using stripping technique to produce random array and apply it in determining electroactive bioanalytes with increased sensitivity and improved selectivity. Scheme 1 depicts the electrochemical fabrication of randomly nanoarrayed nanohole electrodes. The electrodeposition of gold nanoparticles on bare glassy carbon was followed by passivating the surface with polymerization of *in situ* prepared 4-nitro-phenyldiazonium cation. The randomly arrayed nanoholes were produced by stripping the deposited gold nanoparticles as describe in Sceme 1 and an increase in peak current was observed for the

selected probes and cationic drugs compared to current obtained at unmodified glassy carbon electrode.

## **2. Materials and Methods**

### **2.1 Materials**

Para-nitro aniline, C<sub>6</sub>H<sub>6</sub>N<sub>2</sub>O<sub>2</sub> (KIRAN, 99%), sodium nitrite, NaNO<sub>2</sub> (NICE, 96%), hydrochloric acid, HCl (Riedel-De Haen, 37%), potassium tetrachloroaurate (III), KAuCl<sub>4</sub> (Aldrich, 99.995%), hexaminerutheniumchloride (III), Ru(NH<sub>3</sub>)<sub>6</sub>Cl<sub>3</sub> (Aldrich, 98%), sulphuric acid, H<sub>2</sub>SO<sub>4</sub> (Merck, 98%), hydroquinone, C<sub>6</sub>H<sub>6</sub>O<sub>2</sub> (KIRAN, 99%), 2-mercaptoethanol, HSCH<sub>2</sub>CH<sub>2</sub>OH (Aldrich), sodium perchlorate, NaClO<sub>4</sub> (Sigma, 98%+), potassium nitrate, KNO<sub>3</sub> (NICE, 99%), potassium chloride, KCl (FINKEM, 99%), sodium citrate, Na<sub>3</sub>C<sub>6</sub>H<sub>5</sub>O<sub>7</sub>·2H<sub>2</sub>O (FINKEM, 99%), citric acid, (Wardle chemicals ltd, 99%), dopaminehydrochloride (Neon laboratories), chlorpromazinehydrochloride (Emco Laboratory), ascorbic acid, C<sub>6</sub>H<sub>8</sub>O<sub>6</sub> (NICE, 99%), potassium hexacyanoferrate (III), K<sub>3</sub>Fe(CN)<sub>6</sub> (Labmerk Chemicals, 97%) and potassium hydroxide, KOH were of analytical grade reagents and used as received. Distilled water was used to prepare all solutions. Citrate buffer solution was used for preparing drug solutions.

### **2.2 Electrochemical Measurements**

All electrochemical measurements were performed with a BAS-50W electrochemical analyzer (Bioanalytical System Inc. USA model ) and a conventional three-electrode system, comprising a GC working electrode (3 mm), a platinum wire as the auxiliary electrode, and a Ag/AgCl 3.0 mol/L NaCl electrode (from BAS) as reference. All potentials were reported versus the Ag/AgCl reference electrode at room temperature.

### **2.3 Electrode Preparation**

Prior to modification, the bare GC electrode was polished with a fine polishing paper and micro cloth (BAS, Bioanalytical Systems, USA). The electrodes were polished further to a mirror finishing with alumina slurries of 3 μm and 1 μm (BAS, USA) and thoroughly rinsed with distilled water. The electro-conditioning of the GC electrodes was made according to the procedure reported by Soreta and his colleagues [36].

### **2.4 Fabrication of Randomly Nanoarrayed Electrodes**

#### **2.4.1 Electrodeposition of Gold Nanoparticles**

Gold nanoparticles were sequentially electrodeposited on to the conditioned GC electrodes surface according to Soreta et. al. [23]. Shortly, 10 μL of 0.5 mol/L KAuCl<sub>4</sub> was taken in 5 mL of 0.5 mol/L H<sub>2</sub>SO<sub>4</sub> supporting electrolyte in an electrochemical cell. Then chronoamperometry by stepping from 1.10 V for 5 s to deposition potential of 0 V for 5 s in a stirred deposition bath. To increase the number of nanoparticles a three step sequential deposition was done by forming insulation layer using self assembled monolayer of 2-mercaptoethanol on electronucleated gold nanoparticles [23].

#### **2.4.2 Grafting of Nitrophenyl (NP) Film**

The AuNPs modified GC was then grafted with in situ prepared nitrophenyl diazonium cation according to Baranton and his colleagues [26]. Firstly, 100 mL of 3 mmol/L para-nitroaniline in 0.5 mol/L HCl and 10 mL of 0.1 mol/L NaNO<sub>2</sub> were kept separately in an ice jacketed beaker for 1 hr. Then 400 μL of 0.1 mol/L NaNO<sub>2</sub> was added to 20 mL of 3 mmol/L paranitroaniline (PNA) in 0.5 mol/L HCl under stirring at room temperature and CV was used to graft nitrophenyl film on gold nanoparticles (AuNPs) nucleated on GC surface and on the remaining electrode surface not covered with gold nanoparticles in a potential window of -0.2 V to 0.6 V at a scan rate of 0.1 V/s for 3 cycles.

#### **2.4.3 Stripping of Nucleated Gold Nanoparticles**

Nanoholes were produced by stripping the electronucleated AuNPs in 0.1 mol/L KCl using CV scans in a potential range of 0 mV to 1400 mV for three cycles.

#### **2.5 Electrochemical Characterization of Randomly Nanoarrayed Electrodes**

The prepared electrodes were electrochemically characterized by CV using hydroquinone (HQ) and hexamine rutheniumchloride (III), Ru(NH<sub>3</sub>)<sub>6</sub>Cl<sub>3</sub> probes. The signal enhancement of nanoholes was compared to that of a bare GC at both lower and higher scan rates. The radius of the nano holes were also estimated using the obtained data and reported literature values.

#### **2.6 Preparation of solutions of the drugs analysed**

Stock solutions of AA ( $2.0 \times 10^{-3}$  mol/L), DA ( $2.0 \times 10^{-3}$  mol/L) and CPZ ( $2.0 \times 10^{-3}$  mol/L) were prepared in 0.1 mol/L citrate buffer solution, pH 6.5. Citrate buffer was prepared by mixing 0.10 mol/L sodium citrate and 0.10 mol/L citric acid stock solutions using distilled water. The pH values were adjusted by addition of 0.1 mol/L HCl or 0.1 mol/L KOH solutions. Lower concentration of the drugs were prepared by dilution of stock solutions in citrate buffer solution, pH 6.5. Differential pulse voltammetry (DPV) was used for detection of the drugs. For calibration plots of the drugs, average values of three measurements were taken for each concentration.

### **3. Results and Discussion**

#### **3.1 Chronoamperometric Deposition of Gold**

The cyclic voltammogram of 1 mmol/L KAuCl<sub>4</sub> in 0.5 mol/L H<sub>2</sub>SO<sub>4</sub> supporting electrolyte using glassy carbon electrode was similar to the result reported by Soreta et.al. [23]. The deposition of gold on the electrode was confirmed by linear scan voltammetry scan from 1.6 V to 0 V in 0.5 mol/L H<sub>2</sub>SO<sub>4</sub> that showed sharp cathodic peak at 920 mV [23] corresponding to gold oxide reduction. AuNPs were deposited on polished GC chronoamperometrically from stirred 0.1 mmol/L KAuCl<sub>4</sub> in 0.5 mol/L H<sub>2</sub>SO<sub>4</sub> at applied potential of 0 V for 5 s [23]. To increase the number of particles while preventing secondary nucleation, a sequential deposition technique as depicted in Scheme 1 was used with slight modification to that reported by Soreta and his colleagues [23]. The major steps in electrode fabrication are sequential electrodeposition of gold nanoparticles (to increase the number of electronucleated nanoparticles), surface passivation the whole electrode surface by grafting of in situ generated diazonium cation and stripping of nucleated gold nanoparticles. To increase the

number of deposited metal nanoparticles, the already nucleated particles need to be protected to limit the growth of the nuclei to nanometer range hence an alkane thiol of 2-mercaptoethanol that spontaneously adsorbs on gold surfaces [24, 25]. The strong interaction between gold and sulphur was used for controlling and manipulating the reactivity at the surface.

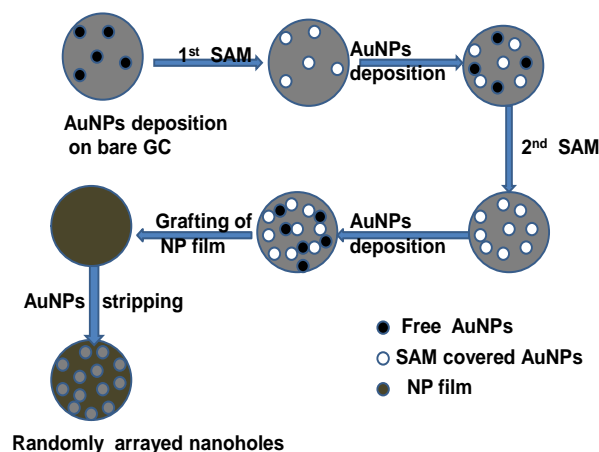


**Figure 1:** Major steps followed in fabrication of randomly nanoarrayed electrodes.

### 3.2 Formation of Nitrophenyl Film and its Electrochemical Characterization

Binding of aryl films to carbon electrodes via the electrochemical reduction of the corresponding diazonium salt can be achieved through either potential cycling or a potential step [26]. Cyclic voltammetry was used to investigate the formation and properties of 4-nitrophenyl films on both bare and goldnanoparticles modified glassy carbon surfaces. NP thin film was electrochemically grafted on bare GC by reduction of *in situ* generated NP diazonium cation in a potential window of -0.2 V to 0.6 V at a scan rate of 0.1 V/s for 3 cycles. In the first cycle of 3 mmol/L p-nitroaniline in 0.5 mol/L HCl, there is a reduction peak appearing at 0.159 V on bare GC. In the subsequent scans, the reduction peak disappears and the residual current becomes smaller with repeated scanning. The loss of the cathodic peak is consistent with the behavior of an electrode being passivated by the grafting of a surface film. Hence the continued electrochemical reduction of *in situ* generated nitrophenyl diazonium ion at the surface is increasingly inhibited by the formation of the grafted layer.

One difference between the voltammograms on polished bare GC and AuNPs deposited GC is that the reduction peak for the attachment of the NP diazonium cation onto the AuNPs modified GC electrode for the first scan was shifted anodically at 218 mV relative to GC surface being at +59 mV.

NP film formed on the bare GC and AuNPs modified GC electrodes were analyzed by comparing the cyclic voltammetry of the  $\text{Fe}(\text{CN})_6^{3-}$  redox probe before and after electrografting the NP film. The redox peaks of ferricyanide observed with bare GC electrodes were almost completely suppressed after the surface NP film was bonded to the electrodes. This gave strong evidence that a uniform monolayer which blocked access of

ferricyanide to the electrode had formed on the GC surfaces. The blocking effect of the NP film observed is consistent with those reported by other workers who also observed the disappearance of the voltammetry response of the redox probe [27].

### 3.3 Nanohole Formation

After modifying the AuNPs deposited GC with NP film, the next step was to fabricate nanoholes. This was achieved by stripping the nucleated AuNPs using CV scans from 0 mV to 1400 mV with six cycles at a scan rate of 0.1 V/s in 0.1 mol/L KCl solution. There was a sharp anodic peak current at around 960 mV in the first scan and its magnitude decreased and disappeared for the next cycles indicating complete removal of the deposited AuNPs as depicted in Figure 1. The KCl was used to encourage oxidation of gold during anodic scan and strip away from the electrode by forming soluble  $\text{AuCl}_4^-$  complex that favors removal of deposited AuNPs. The characteristic gold oxide reduction peak was not observed in 0.5 mol/L  $\text{H}_2\text{SO}_4$  solution after the stripping step that assures complete removal of gold from GC surface.

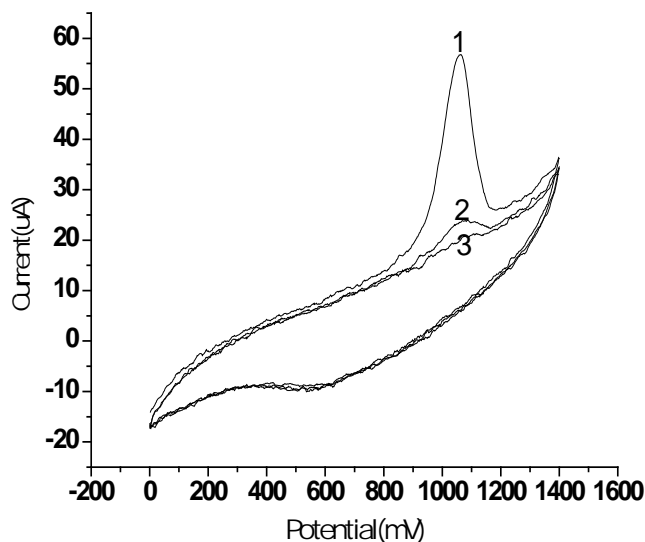


**Figure 2:** Cyclic voltammogram of gold nanoparticles nucleated nitrophenyl modified GC in 0.1 mol/L KCl ( $v = 100$  mV/s). First scan 1, Second scan 2, Third scan 3.

### 3.4 Electrochemical Characterization of Electrodes

Hydroquinone (HQ) and hexamineruthenium chloride (III) were chosen as electrochemical probes to investigate the modified electrodes. Ferrocyanide ion was found to be unsuitable for characterization due to the repulsive forces between the negatively charged NP film and the probe that inhibits its approach to GC electrode surface. The response of HQ is shown in Figure 2.

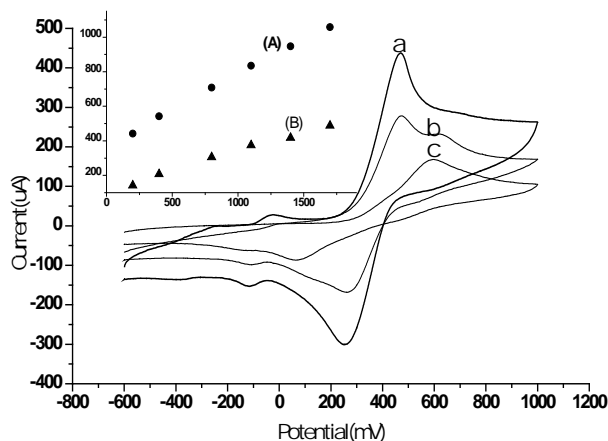


**Figure 3:** CV of 10 mmol/L HQ in 0.1 mol/L NaClO<sub>4</sub> on nitrophenyl (NP) modified nanohole (a), bare GC (b) and nitrophenyl film modified GC (c) (scan rate: 100 mV/s). Inset: A plot of cathodic peak current versus scan rate of 10 mmol/L HQ for nanohole modified GC (A) and bare GC (B).

The current suppression on the NP film modified GC (Figure 2 curve c) arises from decreased density of active sites on the bare GC electrode as some of them are already occupied by the grafted film. But for the NP modified nano hole GC ((Figure 2 curve a), the redox currents have shown good enhancements. However, the possibility of not observing steady state current for nanoelectrode arrays like in our case has been described in literature<sup>[18, 28]</sup>.

Moreover, electrodeposition produces random arrays of nanoparticles on the electrode surface, such that the array rarely, if ever, is diffusionally independent on most practical experimental timescales [10, 17, 19]. However substantial improvement in measured signal and faster mass transport is evident for the randomly nanoarrayed electrodes as compared to be GC.

The inset in Figure 2 shows a plot of cathodic peak current versus scan rate of 10 mmol/L HQ for nanohole modified (A) and bare (B) GC with a linear regression equation of  $I_p (\mu A) = 0.415 V(mV/s) + 365.3$  ( $R=0.999$ ) for the former indicating faster mass transfer and  $I_p(\mu A) = 0.23V(mV/s) + 97.7$  ( $R=0.978$ ) for the later one.

Figure 3 shows the CV response of  $Ru(NH_3)_6^{+3}$  at different scan rates. In comparison with the CV at bare GC electrode, the currents have enhanced values that can be seen from the regression line of  $I (\mu A)$  vs  $V (V/s)$  at NP modified nanohole GC though the actual value will be lesser due to the contribution of the modifier itself. These results suggest that the kinetics/mass transfer of the probes has increased.

As shown in Figure 3 the anodic peak current of 1 mmol/L  $Ru(NH_3)_6^{+3}$  at NP film modified nanohole GC was linearly dependent on the scan rate over the range of 5.12 V/s to 51.2 V/s (instrument limit) with a linear regression equation of  $i(\mu A) = 19.92 (Vs^{-1}) + 342.3$  ( $r = 0.998$ ), (line A) and the peak current also proportional to the square root of scan rate on bare GC in the same range with a linear regression equation of  $i_{pa}(\mu A) = 132.1 Vs^{-1} - 55.64$  ( $r = 0.999$ )



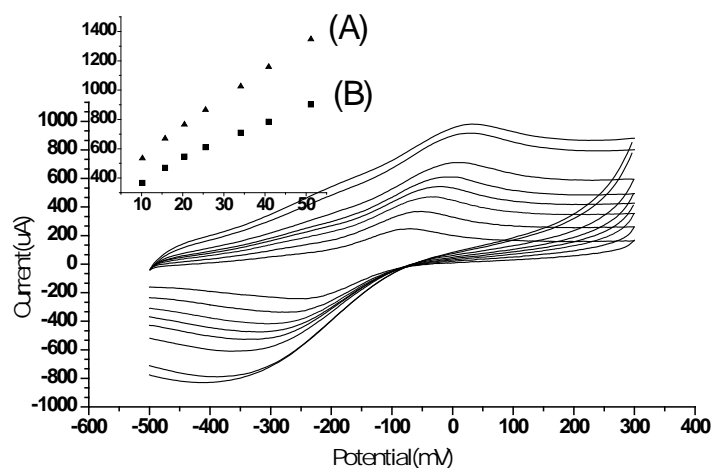


**Figure 4:** Cyclic voltammogram of 1 mmol/L  $\text{Ru}(\text{NH}_3)_6^{+3}$  in 0.1 mol/L  $\text{KNO}_3$  on nitrophenyl modified nanohole GC ( $v = 5.12, 10.24, 15.753, 20.48, 25.6, 34.133, 40.96$  and  $51.2\text{V/s}$  from inner to outer respectively).

The radius of the nanohole produced after stripping the deposited AuNPs was also estimated from the current differences of NP grafted and AuNPs stripped GC (i. e,  $301\ \mu\text{A}$  which was the maximum current difference for  $1\text{mmol/L Ru}(\text{NH}_3)_6^{+3}$ ) at a scan rate of  $40.96\ \text{V/s}$ . According to recessed nanoelectrode model this total current is a multiple of the limiting current of each nanoholes and their total number.

With the adopted procedure, the reported value for the total number of deposited AuNPs for the first round which gave the maximum value per step was  $187/\mu\text{m}^2$  measured over an area of  $48\ \mu\text{m}^2$ . However, for the next two rounds use of SAM of 2-ME gave 127 particles per  $\mu\text{m}^2$  limiting the total number to 314 for 3 rounds [23]. With this value the estimated N value for the geometric electrode area of  $0.84\ \text{cm}^2$  was  $1.56 \times 10^{10}$  particles ( $186 \times 10^8$  particles per  $\text{cm}^2$ ). Using recessed nanoelectrode model with insulation film thickness  $L = 4\ \text{nm}$ , and diffusion coefficient for the redox probe to be equal to  $6.3 \times 10^{-6}\ \text{cm}^2\text{s}^{-1}$  and the limiting current (calculated by dividing maximum current difference with number of nanohole) to be  $1.9 \times 10^{-14}\ \text{A}$ , the radius of the `r` value of 11.5 nm was obtained. This estimates the size of nanoholes to be around 22 nm, a value that falls in the range reported by other authors [29,30] as the average size of deposited AuNPs.

### 3.5 Determination of Dopamine hydrochloride, DA

Detection of DA was made both on bare and NP modified nanohole GC. On the bare GC electrode, the oxidation of DA takes place at around 280 mV and in the reverse scan a reduction peak at 167mV were observed. A well-defined sharp oxidation peak with increased current response was obtained at the nanohole-modified electrode. Eventhough, the response from the NP film modified GC electrode slightly exceeds the response obtained at bare GC, the current measured at these electrodes were smaller than nanohole-modified electrode (inset in Figure 4). The oxidation current of DA was proportional to its concentration over the range  $9.9 \times 10^{-7}\ \text{mol/L}$  to  $3.4 \times 10^{-5}\ \text{mol/L}$  with a correlation coefficient,  $r$  of 0.998 which is significant at  $P=0.05$  (two sided t-test) ( $n=5$ ). The limits of detection for the nanohole modified and bare GC electrodes were  $7.43 \times$

$10^{-8}$  mol/L and  $0.102 \mu\text{mol/L}$ , respectively.

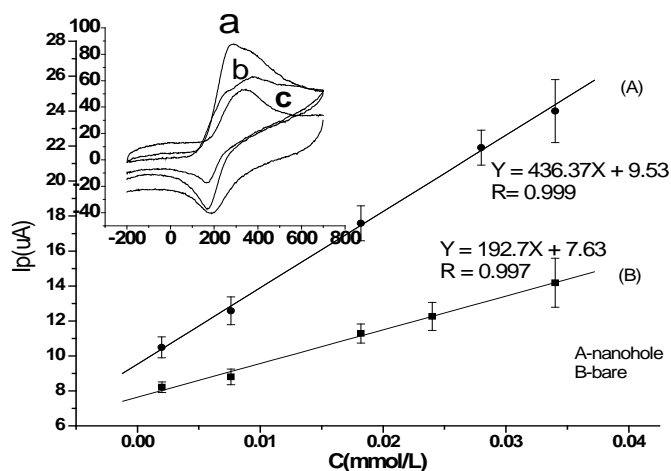


**Figure 5:** Graph of current vs concentration of DA on NP modified nanohole GC (inset: CV of 2 mmol/L DA in 0.1 mol/L citrate buffer (pH 6.5) on NP modified nanohole (a), NP modified (b) and bare (c), GC ( $v = 10\text{mV/s}$ ).

### 3.6 Determination of Ascorbic Acid

At the working pH condition AA exists in the anionic form. Consequently, the NP film repels the negatively charged ascorbate anion and its current response was drastically suppressed over the potential range of interest. This suggested that in addition to the advantage from increased sensitivity, the chemically modified electrode (CME, surface modification is via a covalent bond which is expected to be highly stable) might exhibit useful characteristics for the selective determination of the DA cation in the presence of ascorbate at physiological pH.

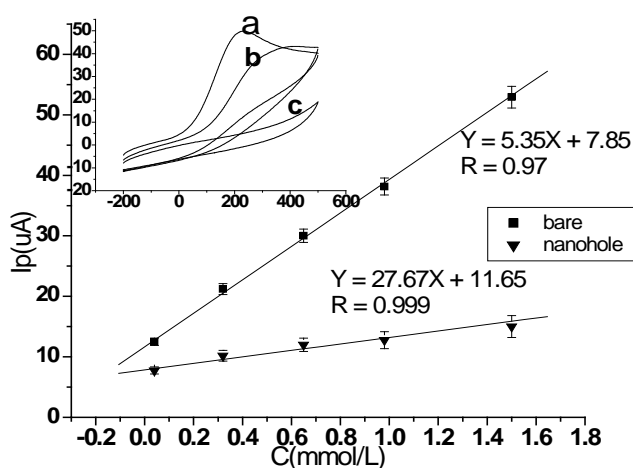


**Figure 6:** Graph of current vs concentration of AA on bare and NP modified nanohole GC (inset : Cyclic voltammogram ( $I(\mu\text{A})$  Vs  $E(\text{mV})$ ) of 2 mmol/L Ascorbic acid in citrate buffer (pH 6.5) on bare (a), NP modified

nanohole (b) & NP modified (c) GC ( $v = 100$  mV/s)

The oxidation peak current on bare GC was linearly dependent on the ascorbate concentration and a linear calibration curve was obtained using DPV in the range of  $0.04 \mu\text{mol/L}$  to  $1.5 \mu\text{mol/L}$  of ascorbate with a correlation coefficient of 0.999, and limit of detection  $0.11 \mu\text{mol/L}$ .

### 3.7 Determination of Chlorpromazine hydrochloride

Chlorpromazine is a central nervous system depressant. The inset in Figure 6 shows its  $2 \text{ mmol/L}$  cyclic voltammogram on bare (a), NP grafted (b) and NP grafted with nanohole (c) GC electrode with peak potentials of  $679 \text{ mV}$ ,  $665 \text{ mV}$  and  $670 \text{ mV}$ , respectively. The increase in current at modified electrode is due to both the decreased capacitive current and cationic nature of the drug<sup>[31-35]</sup> at the working pH condition.

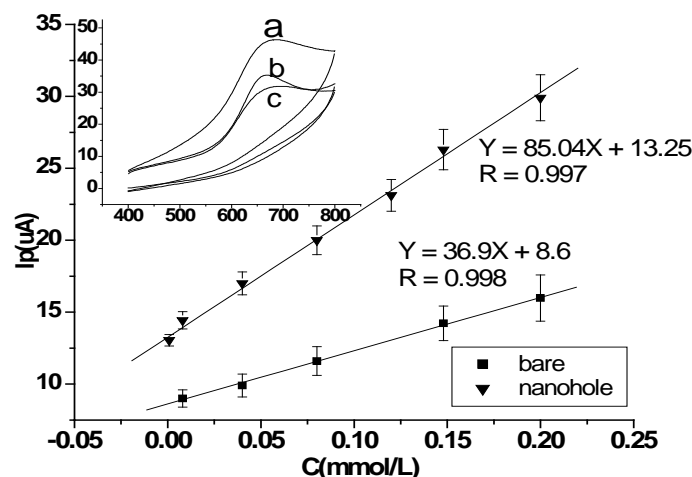


**Figure 7:** Graph of current vs concentration of CPZ on bare and nanohole GC (inset: CV ( $I(\mu\text{A})$  Vs  $E(\text{mV})$ ) of  $2 \text{ mM}$  CPZ in citrate buffer (pH 6.5) on bare (a), NP modified (b), and NP modified nanohole (c) GC ( $v = 100$  mV/s)

The differential pulse voltammetry (DPV) studies showed that the currents of this system depend on the concentration of CPZ. The magnitude of the current for NP modified nanohole GC increased in the presence of CPZ, and proportional to CPZ concentration in the ranges of  $7.96 \times 10^{-6} \text{ mol/L}$  to  $2 \times 10^{-4} \text{ mol/L}$  with the detection limit of  $8.5 \times 10^{-8} \text{ mol/L}$ . The LOD value for bare GC over the same concentration range was  $1.05 \times 10^{-7} \text{ mol/L}$ .

## 4. Conclusion

In this work the fabrication and electrochemical characterization of randomly nanoarrayed electrodes has been presented with exemplified application. Moreover, it is believed that the method presented can be generalized to nanoelectrode arrays of other metals provided that the electronucleation of metallic nanoparticles and effective insulating layer on carbon microspheres is obtained. In addition, the synthesized electrodes were found to have

good characteristics as for the sensing of Dopamine and Chlorpromazine hydrochloride and might be used as a strategy for the selective determination of other electroactive cationic drugs where the anionic species interfere. As long as the calibration curve is precise, such a nanoelectrode array can be employed for detecting trace redox species in environmental monitoring of toxic metal ions and organic molecules, and electrophysiological studies. It is recommended that this study needs to be extended by varying the charge of grafting film and using nano imaging techniques (AFM, SEM...etc) for characterization of the nanoarray electrodes so that a standard procedure can be set for further applications.

### **Acknowledgements**

The authors acknowledge Ethiopian Ministry of Education (MoE), Mettu University and Jimma University for their material and financial support.

### **References**

- [1] J. J. Gooding, M. H. Leo, L. M. H. Lai, Y. Ian, I.Y. Goon." Advances in Electrochemical Science and Engineering." in Nanostructured Electrodes with Unique Properties for Biological and Other Applications., Vol. 1. C. A. Richard, M. Dieter, K. L. Jacek, N. R. Philip, Eds. WILEY-VCH: Weinheim, 2009 p. 415.
- [2] K. Jessica, L. Jun, M. Alan, H. Cassell, Q. Chen, H. T.Ye, H. Jie, M. Meyyappan. "The fabrication and electrochemical characterization of carbon nanotube nanoelectrode arrays." *Journal of Material Chemistry*, vol. 14, pp. 676 – 684, 2004.
- [3] V. M. Mirsky. "New electroanalytical applications of self-assembled monolayers." *Trends in Analytical Chemistry*, vol. 21, pp. 439-450, 2000.
- [4] F. N. Crespilho, V. Zucolotto, O. N. Oliveira, F. C. Nart." Dendrimers as nanoreactors to produce platinum nanoparticles embedded in layer-by-layer films for methanol-tolerant cathodes." *Electrochemistry Communications*, vol. 8, pp. 348-352, 2006.
- [5] P. Ugo, L. M. Moretto, F. Vezza, "Ionomer-coated electrodes and nanoelectrode ensembles as electrochemical environmental sensors: Recent advances and prospects." *ChemPhysChem*, vol. 3, pp. 917-925, 2002.
- [6] X.-J. Huang, Y. K. Choi. "Chemical sensors based on nanostructured materials." *Sensors and Actuators, B* vol. 122, pp. 659-671, 2007.
- [7] M. Penner, C. R. Martin. "Preparation and electrochemical characterization of ultra-micro-electrode ensembles." *Analytical Chemistry*, vol. 59, pp. 2625-2630, 1987.
- [8] W. S. Baker, R. M. Crooks. "Independent Geometrical and Electrochemical Characterization of Arrays

- of Nanometer-Scale Electrodes.” *Journal of Physical Chemistry B*, vol. 102, pp. 10041-10046, 1998.
- [9] W. Royce, R. W. Murray. “Nanoelectrochemistry: Metal Nanoparticles, Nanoelectrodes, and Nanopores.” *Chem. Rev.* vol. 108, pp 2688-2720, 2008.
- [10] N. Godino, X. Borrís, F. X. Muñoz, Compton, R.G.”Mass transport to nanoelectrode arrays and limitations of the diffusion domain approach: Theory and experiment.” *Journal of Physical Chemistry C*, vol. 113, pp. 11119-11125, 2009.
- [11] D. W. M. Arrigan. “Nanoelectrodes, nanoelectrode arrays and their applications.” *Analyst*, vol. 129, pp. 1157-1165, 2004.
- [12] J. P. Kutter, O. Geschke, H. Klank, P. Tellema. *Microfluidics: Theoretical Aspect in microsystem engineering of lab on chip devices*. Wiley, VCH, 2004, p. 452.
- [13] A. O. Simm, S. Ward-Jones, C. E. Banks, R. G. Compton. “Novel methods for the production of silver microelectrode-arrays: their characterization by atomic force microscopy and application to the electroreduction of halothane.” *Anal. Sci.*, vol. 21, pp. 667-671, 2005.
- [14] C. G. Zoski. “Ultra microelectrodes: Design, Fabrication, and Characterization.” *Electroanalysis*, vol.14, pp. 1041-1051, 2002.
- [15] A. J. Bard, M.V. Mirkin. *Scanning Electrochemical Microscopy*, Marcel Dekker, Inc: United States of America 2001, p. 650.
- [16] V. P. Menon, C. R. Martin. “Fabrication and evaluation of nanoelectrode ensembles.” *Anal. Chem.*, vol. 67, pp. 1920-1928, 1995.
- [17] N. Triroj, P. Jaroenapibal, H. Shi, J. I. Yeh, R. Beresford. “Microfluidic chip-based nanoelectrode array as miniaturized biochemical sensing platform for prostate-specific antigen detection.” *Biosensors and Bioelectronics*, vol. 26, pp. 2927-2933, 2011.
- [18] M. S. Doescher, U. Evans, P.E. Colavita, P. G. Miney, M. L. Myrick. “Construction of a nanowell electrode array by electrochemical gold stripping and ion bombardment.” *Electrochemical and Solid-State Letters*, vol. 6, pp. 112-115, 2003.
- [19] L. Xiao, I. Streeter, G. G. Wildgoose, R. G., Compton. “Fabricating random arrays of boron doped diamond nano-disc electrodes: Towards achieving maximum Faradaic current with minimum capacitive charging.” *Sensors and Actuators B*, vol. 133, pp. 118-127, 2008.
- [20] H. Liu, Y. Tian, P. Xia. “Pyramidal, rodlike, spherical gold nanostructures for direct electron transfer of copper, zinc-superoxide dismutase: application to superoxide anion biosensors.” *Langmuir*, vol. 24, pp. 6359-6366, 2008.

- [21] L. C. Giancarlo, G. W. Flynn. "Scanning tunneling and atomic force microscopy probes of self-assembled, physisorbed monolayers: peeking at the peaks." *Annual Review of Physical Chemistry*, vol. 49, pp. 297-336, 1998.
- [22] L. L. Kesmodel, L. H. Dubois, G. A. Somorjai. "Dynamical LEED Study of C<sub>2</sub>H<sub>2</sub> and C<sub>2</sub>H<sub>4</sub> Chemisorption of Pt(111): Evidence for the Ethylidyne (-C-CH<sub>3</sub>) Group." *Chem. Phys. Lett.*, vol. 56, pp. 267-271, 1978.
- [23] T. R. Soreta, J. Strutwolf and C. K. O'Sullivan. "Electrochemical Fabrication of Nanostructured Surfaces for Enhanced Response." *Chemphyschem*, vol. 9, pp. 920-927, 2008.
- [24] H. O. Finklea. "Electrochemistry of organized monolayers of thiols and related molecules on electrodes" in *Electroanalytical Chemistry*, Vol. 19, Bard, A. J., Rubinstein, I., Eds., New York: Marcel Dekker, 1996, pp. 109-335.
- [25] R. K. Smith, P. A. Lewis and P. S. Weiss. "Patterning self-assembled monolayers." *Progress in Surface Science*, vol. 75, pp. 1-68, 2004.
- [26] S. Baranton, D. Belanger. "Electrochemical Derivatization of Carbon Surface by Reduction of in Situ Generated Diazonium Cations." *J. Phys. Chem. B*, vol. 109, pp. 24401-24410, 2005.
- [27] C. Saby, B. Ortiz, G. Y. Champagne, D. Belanger. "Electrochemical modification of glassy carbon electrode using aromatic diazonium salts. 1. Blocking effect of 4-nitrophenyl and 4-carboxyphenyl groups." *Langmuir*, vol. 13, pp. 6805-6813, 1997.
- [28] L. M. Moretto, M. Tormenb, A. Carpentierob, P. Ugo. "Arrays of nanoelectrodes: Critical evaluation of geometrical and diffusion characteristics with respect to electroanalytical applications." *ECS Transactions*, vol. 25, pp. 33-38, 2010.
- [29] F. Mirkhalf, K. Tammeveski, D. J. Schiffrin. "Electrochemical reduction of oxygen on nanoparticles gold electrodeposited on a molecular template." *PhyChemChemPhy.*, vol. 11, pp. 3463-3471, 2009.
- [30] F. M. El-Cheick, F. A. Rashwan, H. A. Mahmoud, M. El-Rouby. "Gold nanoparticle-modified glassy carbon electrode for electrochemical investigation of aliphatic di-carboxylic acids in aqueous media." *J. Solid State Electrochem.*, vol. 14, pp. 1425-1443, 2010.
- [31] X. Xi, L. Ming, J. Liu. "Voltammetric determination of promethazine hydrochloride at a multi-wall carbon nanotube modified glassy carbon electrode." *Drug Testing and Analysis*, vol. 3, pp. 182-186, 2011.
- [32] J. Strutwolf and C. K. O'Sullivan. "Microstructures by selective desorption of self-assembled monolayer from polycrystalline gold electrodes." *Electroanalysis*, vol. 19, pp. 1467-1475, 2007.

- [33] R. N. Goyal, V. K. Gupta, M. Oyama, N. Bachheti. "Gold nanoparticles modified indium tin oxide electrode for the simultaneous determination of dopamine and serotonin: Application in pharmaceutical formulations and biological fluid." *Talanta*, vol.72, pp. 976-983, 2007.
- [34] F. Malem, D. Mandler."Self Assembled Monolayers in Electroanalytical Chemistry: Application of Mercapto Carboxylic Acid Monolayers for the Electrochemical Detection of Dopamine in the Presence of a High Concentration of Ascorbic Acid." *Anal. Chem.*, vol. 65, pp. 37-41, 1993.
- [35] Y. Ni, L. Wanga, S. Kokot. "Voltammetric determination of chlorpromazine hydrochloride and promethazine hydrochloride with the use of multivariate calibration." *Analytica Chimica Acta*, vol. 439, pp. 159-168, 2001.
- [36] T. R. Soreta, J. Strutwolf and C. K. O'Sullivan. "Electrochemically deposited palladium as a substrate for self-assembled monolayers." *Langmuir*, vol. 23, pp. 10823-10830, 2007.